Correlation of Myocardial *p*-^{123}I-Iodophenylpentadecanoic Acid Retention with ^{18}F-FDG Accumulation During Experimental Low-Flow Ischemia

Cindy Q. Shi, MD[1]; Lawrence H. Young, MD[1]; Edouard Daher, MD[1]; Edward V.R. DiBella, PhD[2]; Yi-Hwa Liu, PhD[1]; Eliot N. Heller, MD[1]; Sami Zoghbi, PhD[3]; Frans J.Th. Wackers, MD[1,3]; Robert Soufer, MD[1,4]; and Albert J. Sinusas, MD[1,3]

[1]Experimental Nuclear Cardiology Laboratory, Division of Cardiovascular Medicine, Department of Internal Medicine, Yale University School of Medicine, New Haven, Connecticut; [2]Department of Radiology, University of Utah, Salt Lake City, Utah; [3]Department of Diagnostic Radiology, Yale University School of Medicine, New Haven, Connecticut; and [4]Positron Imaging Laboratory, Yale University/Department of Veteran Affairs, West Haven, Connecticut

Myocardial ischemia is associated with reduced free fatty acid (FFA) β-oxidation and increased glucose utilization. This study evaluated the potential of dynamic SPECT imaging of a FFA analog, *p*-^{123}I-iodophenylpentadecanoic acid (IPPA), for detection of ischemia and compares retention of IPPA with ^{18}F-FDG accumulation. **Methods:** In a canine model of regional low-flow ischemia ($n = 9$), serial IPPA SPECT images (2 min per image) were acquired over 52–90 min. In a subset of dogs ($n = 6$), ^{18}F-FDG was injected after completing SPECT imaging and allowed to accumulate for 40 min before killing the animals. Flow was assessed with radiolabeled microspheres. Myocardial metabolism was evaluated independently by selective coronary arterial and venous sampling. **Results:** Serial IPPA SPECT images showed an initial defect in the ischemic region (0.70% ± 0.03% ischemic-to-nonischemic ratio), which normalized within 48 min because of the slower IPPA clearance from the ischemic region ($t_{1/2} = 54.2 \pm 3.3$ min) relative to the nonischemic region ($t_{1/2} = 36.7 \pm 5.6$ min) ($P < 0.05$). Delayed myocardial IPPA and ^{18}F-FDG activities were correlated ($r = 0.70$; $n = 576$ segments), and both were maximally increased in segments with a moderate flow reduction (IPPA, 151% of nonischemic; ^{18}F-FDG, 450% of nonischemic; $P < 0.05$). **Conclusion:** Serial SPECT imaging showed delayed myocardial clearance of IPPA in ischemic regions with moderate flow reduction, which lead to increased late myocardial retention of IPPA. Retention of IPPA correlated with ^{18}F-FDG accumulation, supporting the potential of IPPA as a noninvasive marker of ischemic myocardium.

Key Words: *p*-^{123}I-iodophenylpentadecanoic acid; ^{18}F-FDG; radionuclide imaging; myocardium; ischemia; fatty acids; metabolism; iodinated fatty acid

J Nucl Med 2002; 43:421–431

Received Apr. 2, 2001; revision accepted Dec. 3, 2001.

For correspondence or reprints contact: Albert J. Sinusas, MD, Nuclear Cardiology, Yale University School of Medicine, P.O. Box 208017, 333 Cedar St., 3FMP, New Haven, CT 06520-8017.

E-mail: Albert.Sinusas@yale.edu

Noninvasive approaches for the detection of myocardial ischemia have generally been based on either the detection of flow heterogeneity or the identification of regional alterations of myocardial metabolism. PET has become a standard for determination of regional glycolytic metabolism in evaluation of patients with ischemic heart disease. Ischemic myocardium can be identified by the accumulation of ^{18}F-FDG, a marker of exogenous glucose utilization (*1*,*2*). Analysis of ^{11}C-palmitate clearance was also proposed to identify ischemic myocardium (*3–5*), although the efficacy of ^{11}C-palmitate may have been partially limited by incorporation of the tracer into triglyceride pools and backdiffusion of nonmetabolized tracer (*6*). Although widespread implementation of PET imaging for assessment of myocardial metabolism has also been limited by availability and expense, analysis of either glucose or fatty acid metabolism may still have clinical usefulness for the noninvasive assessment of ischemic myocardium.

Efforts have been directed toward the development of iodinated fatty acids, which can be imaged with standard SPECT. *p*-^{123}I-Iodophenylpentadecanoic acid (IPPA) is a radiolabeled free fatty acid (FFA) analog that has a phenyl group substituted at the ω-carbon of palmitic acid, stabilizing the iodine on the molecule and inhibiting β-oxidation of the terminal end of the compound (*7*,*8*). This modification prolongs myocardial clearance, reduces the release of free iodine by myocardial and hepatic metabolism, and results in most of the IPPA metabolites being readily excreted by the kidney. Maximal uptake of IPPA by myocardium is considerably greater than that of palmitic acid (*9–11*), and IPPA images show minimal background activity and improved image quality (*9*). The initial clearance of IPPA parallels that of palmitic acid (*9–11*) and is thought to reflect β-ox-

idation (*9*). The late clearance is of IPPA is thought to reflect clearance of tracer incorporated into triglyceride pools (*9*).

In experimental models of reperfused infarctions and clinical studies, IPPA displays delayed uptake and clearance from ischemic or infarcted myocardium (*12–18*). In a recent study, myocardial IPPA clearance was also evaluated during experimental low-flow ischemia using serial planar imaging (*19*). IPPA showed nearly complete redistribution over 2 h, but this study was limited in that SPECT imaging was not used, absolute regional IPPA clearance was not evaluated, and the retention of IPPA was not related to any other markers of metabolism.

We hypothesized that decreased myocardial FFA oxidation during low-flow ischemia would lead to decreased early clearance of IPPA and a late increase in relative myocardial retention. Myocardial ischemia results not only in a reduction in β-oxidation of fatty acids (*20,21*) but also accelerated glucose uptake, a substrate for anaerobic metabolism (*20,22*). Therefore, we also hypothesized that the late relative myocardial retention of IPPA under ischemic conditions would correspond to increased accumulation of ^{18}F-FDG.

The goals of this study were to (a) evaluate the potential of dynamic IPPA SPECT imaging for the detection of ischemia, using monoexponential fitting of myocardial clearance curves to estimate IPPA clearance, and (b) compare the late relative myocardial retention of IPPA and ^{18}F-FDG as a function of myocardial blood flow.

MATERIALS AND METHODS

This study was conducted with the approval of the Yale Animal Care and Use Committee in compliance with the guiding principles of the American Physiological Society on research animal use. Experiments were performed on 11 fasting adult mongrel dogs of either sex. All dogs were anesthetized with sodium thiamylal (20 mg/kg intravenously), intubated, and mechanically ventilated with a mixture of halothane (0.5%–1.5%), nitrous oxide, and oxygen (N_2O:O_2 = 3:1).

Experimental Preparation

The experimental preparation has been reported (*23*) and is briefly outlined below. One femoral vein and both femoral arteries were isolated and cannulated for administration of fluids, radiotracers, pressure monitoring, and arterial blood sampling. A left lateral thoracotomy was performed for cardiac instrumentation (Fig. 1). A catheter was placed in the left atrium for injection of radiolabeled microspheres. A micromanometer catheter (Millar Instruments, Inc., Houston, TX) was passed through the carotid artery into the left ventricle for measurement of pressure and the first derivative of pressure (dP/dt). The proximal left anterior

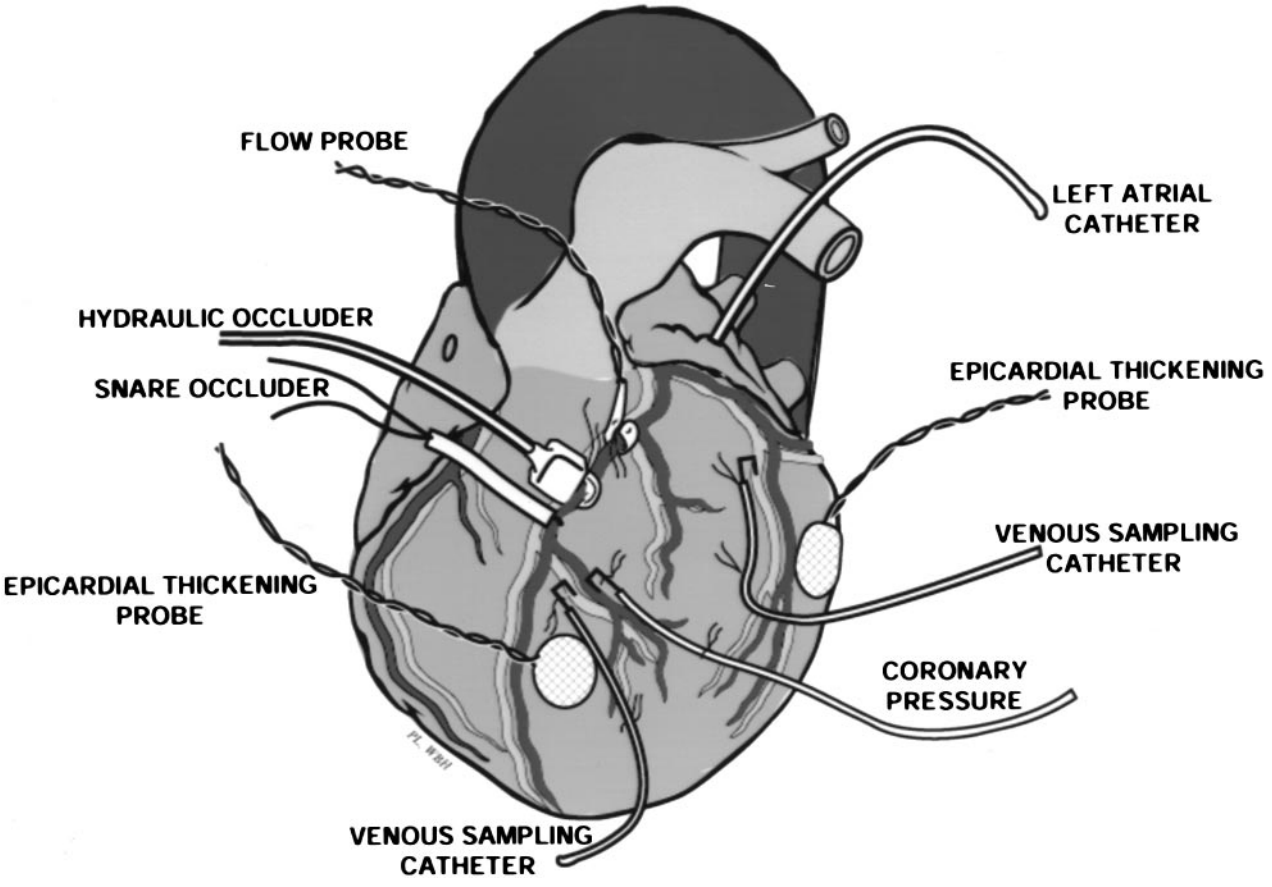

FIGURE 1. Surgical instrumentation of heart.

descending coronary artery (LAD) was isolated after the first major diagonal branch for placement of a hydraulic occluder (model VO-3; Rhodes Medical Instruments, Woodland Hills, CA). Doppler transducers (10 MHz; Crystal Biotech, Hopkinton, MA) were attached to the epicardium of the left ventricle for measurement of regional myocardial thickening (*24*) on the anterior wall distal to the occluder and on the posterolateral wall.

The distal LAD was cannulated with a specially designed catheter that permits monitoring of distal coronary pressure without compromise of flow (*23*). The anterior cardiac and obtuse marginal veins were cannulated using similar catheters for selective venous sampling from the central ischemic and nonischemic regions.

Experimental Protocol

The experimental protocol is summarized in Figure 2. Hemodynamics were monitored continuously and recorded every 5 min using a data acquisition software package (Dataflow; Crystal Biotech). After 30 min of baseline measurements, a partial stenosis of the LAD was established by adjusting the hydraulic occluder to maintain the distal LAD mean pressure at approximately 50% of mean aortic pressure throughout the period of stenosis. After 60 min of steady-state low-flow ischemia, IPPA (185 MBq) was injected intravenously over 20 s. Serial arterial samples were taken after the IPPA injection for determination of blood IPPA clearance. Serial 2-min in vivo SPECT images were acquired over 52–90 min to evaluate myocardial clearance of IPPA. After 150 min of ischemia, after completion of the IPPA imaging, approximately 111 MBq ^{18}F-FDG were injected intravenously in 7 of 11 dogs that were killed 40 min later. Four of the 11 dogs were not injected with ^{18}F-FDG, although they were killed at the same time after IPPA injection.

Arterial and venous blood from the ischemic LAD and control left circumflex artery (LCX) regions was sampled (~3 mL) during baseline, stenosis, and just before injections of IPPA and ^{18}F-FDG. At corresponding times, regional blood flow was also assessed with radiolabeled microspheres.

Measurement of Myocardial Thickening

Myocardial thickening was assessed in the central ischemic and the nonischemic regions with nontraumatic pulsed single-crystal Doppler epicardial transducers as reported (*24*). The thickening fraction was calculated by dividing the transmural net systolic thickening by the end-diastolic wall thickness, estimated by the range depth, and expressed as a percentage.

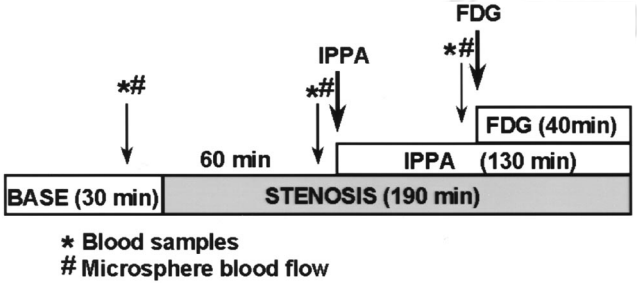

FIGURE 2. Experimental protocol. After baseline (BASE) measurements, partial coronary stenosis was created and maintained throughout protocol. Arterial and venous samples were obtained for metabolic measurements, and radiolabeled microspheres were injected at times designated. IPPA was injected 60 min after creation of stenosis. ^{18}F-FDG was injected 90 min later.

Measurement of Myocardial Blood Flow

Radiolabeled (^{113}Sn, ^{103}Ru, ^{95}Nb, ^{46}Sc, and ^{51}Cr) microspheres (11-μm mean diameter; 2–12 million) were injected into the left atrium at the end of baseline and during the stenosis immediately before injection of IPPA and ^{18}F-FDG. Paired reference samples of arterial blood were withdrawn through a roller pump from both femoral arteries for the calculation of myocardial blood flow according to standard methods (*25*).

Measurement of Myocardial Metabolism

Blood oxygen content was measured during the experiment using a hemoximeter (Osm3; Radiometer Copenhagen, Copenhagen, Denmark). Blood lactate was measured using an automated lactate oxidase method (Yellow Springs Instruments, Yellow Springs, OH). Oxygen consumption (mL O_2/min/100 g) and lactate balance (μmol/min/100 g) were assessed by combining measurements of arterial and venous concentration differences and average myocardial microsphere blood flow, in the relevant central ischemic and nonischemic regions. Plasma FFA was measured by a microfluorometric method (*26*). Regional coronary plasma flow was calculated using measures of transmural microsphere flow in the region of selective sampling and estimated hematocrit. The myocardial FFA uptake was calculated from the concentration difference and estimated coronary plasma flow.

IPPA and ^{18}F-FDG

IPPA was supplied by a commercial vendor (Nordion International Inc., Vancouver, Canada) or prepared at our institution using the precursor phenylpentadecanoic acid provided by the same vendor. Radioiodination was performed using the organothallium intermediate according to published methods (*27*). The radiochemical purity of the preparations as determined by extraction into diethyl ether was 97.8% ± 0.4%; specific activity was approximately 1,410 ± 11.1 MBq/mg.

^{18}F-FDG (specific activity, >185 GBq/mmol) was prepared in an 11-MeV negative-ion cyclotron (CTI, Knoxville, TN).

Acquisition and Analysis of Serial IPPA SPECT Imaging

Serial IPPA SPECT images were acquired with a triple-head gamma camera (Prism 3000; Picker International, Cleveland Heights, OH). Serial SPECT images (2 min each) were acquired using a high-resolution, low-energy, parallel-hole collimator, 64 × 64 matrix size, and 1.42 zoom. A 20% energy window was centered at the 159-keV photopeak of ^{123}I. No attenuation or scatter corrections were made during processing.

Images were reconstructed using standard filtered backprojection. Reconstructed SPECT short-axis images (5-mm thick) were generated and quantified using a previously reported and validated approach (*28,29*). Circumferential maximal count profiles were generated. The orientation of the short-axis SPECT images was visually matched with the postmortem microsphere data, which was expressed for 8 radial sectors per slice. Regions of interest were generated semiautomatically from the short-axis slices. Time–activity curves were generated from 4 regions in each slice, starting at 4 min after injection and continuing to 52–90 min after injection. Data acquired during the first 8 min of image acquisition were discarded from the regional clearance analysis because these images were contaminated by substantial blood-pool activity and IPPA was still washing in. Time–activity curves were fit to a monoexponential ($A = A_0e^{-kt}$). The time required for half of the activity to wash out was calculated for each region ($t_{1/2} = 0.693/k$). The washout parameters from each region were bilinearly inter-

TABLE 1
Hemodynamic Data

Parameter	HR (bpm)	AOP (mm Hg)	LADP (mm Hg)
Baseline	105 ± 7	97 ± 8	93 ± 9
Stenosis 60 min*	107 ± 9	89 ± 9	49 ± 8†
Stenosis 150 min‡	105 ± 9	80 ± 8	47 ± 7†

*After 60 min of low-flow ischemia.
†$P < 0.05$ vs. baseline.
‡After 150 min of low-flow ischemia.
HR = heart rate; AOP = mean aortic pressure; LADP = left anterior descending pressure, distal to stenosis; bpm = beats per minute.
$n = 9$ dogs.

polated into a polar map. Regions of interests were chosen to delineate the defect region and a normal region on the short-axis slices. These SPECT regions were selected on the basis of microsphere blood flow in matched postmortem slices.

Postmortem Analysis

After killing the animals, the hearts were divided from base to apex into 4 slices of equal thickness (1- to 1.5-cm thick). The slices were incubated in a buffered solution of triphenyltetrazolium chloride (TTC) for 15 min at 37°C to 39°C to evaluate for myocardial necrosis.

Myocardial Blood Flow and IPPA and ^{18}F-FDG Activity

Each myocardial slice was cut into 8 radial sectors, which were subdivided into epicardial, midwall, and endocardial segments, resulting in a total of 96 segments per heart for quantification of myocardial IPPA activity, ^{18}F-FDG activity, and blood flow. Myocardial ^{18}F-FDG activity was measured immediately after cutting the tissue, using a γ-well autoscintillation counter (Cobra 5003; Packard Instrument Co., Downers Grove, IL). Myocardial IPPA activity was determined by recounting the tissue 24 h later, after decay of ^{18}F-FDG. The samples were counted a third time for determination of microsphere flow 5 d after killing, after decay of IPPA. Separation of isotopes by energy windows was performed according to standard published methods using decay correction and spill-up and spill-down correction (*23–25*).

Myocardial IPPA and ^{18}F-FDG activity in the ischemic region was expressed as a percentage of the central nonischemic LCX region to facilitate comparisons between dogs (*25*). Because of the heterogeneity of flow within the ischemic region, myocardial IPPA and ^{18}F-FDG retained activity was related to the extent of flow reduction as determined by microspheres. Segments were divided arbitrarily into categories on the basis of the microsphere blood flow (≤20%, 21%–40%, 41%–60%, 61%–80%, 81%–100%, and >100%).

Statistical Analysis

All data are presented as mean ± SEM. Comparisons between 2 groups were made using either a paired or unpaired Student *t* test. If multiple comparisons were performed, a Dunnett multiple comparison test was used. Differences between groups were considered significant at $P < 0.05$ (2-tailed).

RESULTS

The surgical preparation was conducted on 11 dogs (average weight, 22.3 ± 1.1 kg). One animal died of ventricular fibrillation during surgery. One additional dog was excluded from the analysis because myocardial infarction was evident from postmortem TTC staining.

Hemodynamics

Hemodynamic data are summarized in Table 1 for the 9 surviving dogs without myocardial infarction. No significant change in heart rate occurred during partial stenosis of the LAD. However, aortic pressure tended to decrease and was mildly reduced after 150 min of low-flow ischemia. The coronary stenosis reduced distal mean coronary artery pressure by 53%, resulting in a pressure gradient across the stenosis of approximately 40–50 mm Hg relative to the mean aortic pressure.

Regional Myocardial Thickening

Thickening fractions in central ischemic and nonischemic regions are summarized in Table 2. Partial occlusion of the LAD led to severe hypokinesis in the central ischemic area, which persisted throughout the ischemic period. The thickening fraction in the posterior nonischemic region was lower than that in the anterior region at baseline but did not change during anterior ischemia.

Regional Myocardial Blood Flow

When myocardial blood flow in the ischemic region was expressed as a percentage of the nonischemic flow, there was a consistent reduction in average transmural flow in the ischemic region at the times of IPPA (60 min, 67.7% ± 3.5% of nonischemic) and ^{18}F-FDG (150 min, 70.2% ± 3.5% of nonischemic) injections (Fig. 3). This 30% reduction in relative transmural myocardial flow was associated with an approximately 55% reduction in endocardial flow in the ischemic regions during the stenosis.

Changes in absolute myocardial blood flow (mL/min/g) in the central ischemic and nonischemic regions are summarized in Table 3. During the partial stenosis there was a significant reduction of flow in the endocardium and a trend

TABLE 2
Thickening Fraction in Central Ischemic and Nonischemic Regions

Parameter	Thickening fraction (%)	
	Ischemic (LAD)	Nonischemic (LCX)
Baseline	19.8 ± 2.0	11.8 ± 1.3
Stenosis 60 min*	5.5 ± 1.9†	12.0 ± 1.3
Stenosis 150 min‡	4.7 ± 2.1†	10.5 ± 1.9

*After 60 min of low-flow ischemia.
†$P < 0.05$ vs. baseline.
‡After 150 min of low-flow ischemia.
$n = 9$ dogs.

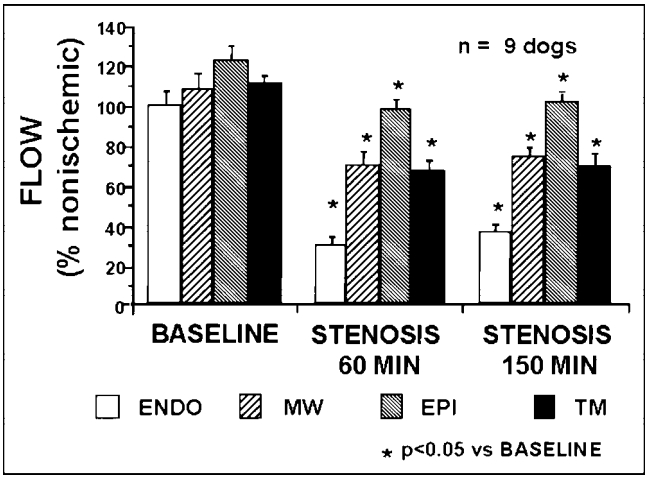

FIGURE 3. Myocardial blood flow in endocardial (ENDO), midwall (MW), epicardial (EPI), and transmural (TM) layers of central ischemic region are expressed as percentage of nonischemic region. Normalized flows are shown at baseline and at time of IPPA (stenosis 60 min) and ^{18}F-FDG (stenosis 150 min) injections.

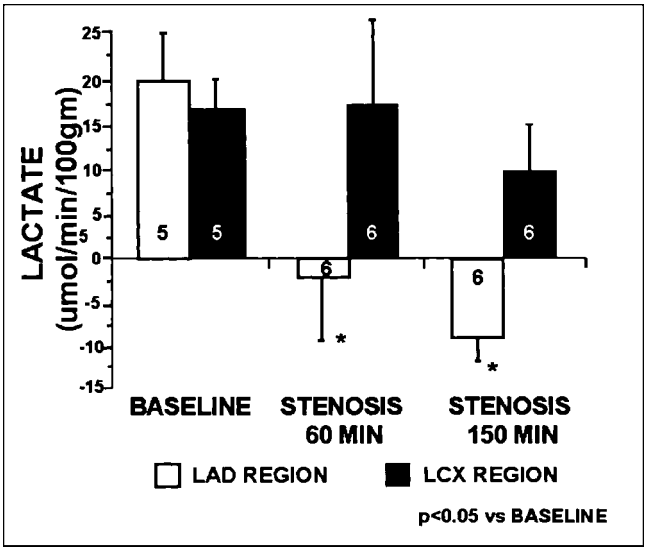

FIGURE 4. Lactate balance for LAD and LCX was measured during baseline and after 60 min (stenosis 60 min) and 150 min (stenosis 150 min) of partial coronary occlusion. Time points correspond to time of IPPA and ^{18}F-FDG injections.

toward lower midwall flows. Epicardial flows were unchanged. Overall, there was a significant reduction in transmural flow in the ischemic region at 150 min after creation of the stenosis. Although absolute transmural myocardial blood flow at the time of IPPA injection tended to be slightly higher than that during the ^{18}F-FDG injections, this difference was not statistically significant.

Myocardial Metabolism

The arterial lactate concentration was 0.9 ± 0.1 mmol/L at baseline and remained stable during the stenosis (150 min). Net myocardial lactate uptake was found in LAD and LCX regions before the stenosis (Fig. 4). Significant net lactate production from the central ischemic region occurred after creation of the stenosis ($P < 0.05$ vs. baseline), confirming accelerated anaerobic glycolytic metabolism during low-flow ischemia.

Myocardial oxygen consumption in the LAD region (expressed as percentage of the nonischemic region) was reduced by 25% at 60 min after stenosis ($P < 0.01$ vs. baseline) and by 45% at 120 min after stenosis ($P < 0.01$ vs. baseline) (Table 4). Thus, oxygen consumption remained depressed throughout the period of stenosis.

Arterial FFA concentration was 0.9 ± 0.2 mmol/L and stayed constant. FFA uptake in the ischemic region (expressed as percentage of the nonischemic region) was reduced 39% ($P < 0.05$ vs. baseline) at the time of IPPA injection and was reduced 41% ($P < 0.05$ vs. baseline) at the time of ^{18}F-FDG injection. Thus, FFA uptake in the

TABLE 3
Microsphere Flow in Central Ischemic and Nonischemic Regions

Parameter	Flow (mL/min/g)			
	Endocardial	Midwall	Epicardial	Transmural
Ischemic (LAD)				
Baseline	0.75 ± 0.11	0.78 ± 0.10	0.92 ± 0.13	0.82 ± 0.11
Stenosis 60 min*	0.34 ± 0.07†	0.69 ± 0.11	0.99 ± 0.14	0.67 ± 0.10
Stenosis 150 min‡	0.29 ± 0.05†	0.58 ± 0.11	0.83 ± 0.13	0.56 ± 0.09†
Nonischemic (LCX)				
Baseline	0.76 ± 0.12	0.75 ± 0.11	0.76 ± 0.11	0.76 ± 0.11
Stenosis 60 min*	0.98 ± 0.14	0.97 ± 0.14	1.01 ± 0.15	0.99 ± 0.14
Stenosis 150 min‡	0.87 ± 0.18	0.84 ± 0.17	0.83 ± 0.13	0.84 ± 0.16

*After 60 min of low-flow ischemia.
†$P < 0.05$ vs. baseline.
‡After 150 min of low-flow ischemia.
$n = 9$ dogs.

TABLE 4
Regional Oxygen Consumption (MVO_2) and FFA Uptake in Central Ischemic Region

Parameter	MVO_2* (% nonischemic)	FFA† (% nonischemic)
Baseline	101.4 ± 12	115.4 ± 5.5
Stenosis 60 min‡	76.4 ± 3.3§	70.0 ± 7.9§
Stenosis 150 min‖	55.3 ± 12.1§	68.3 ± 5.0§

*n = 9 dogs.
†n = 5 dogs.
‡After 60 min of low-flow ischemia.
§$P < 0.01$ vs. baseline.
‖After 150 min of low-flow ischemia.

ischemic region remained uniformly depressed throughout the period of low-flow ischemia (Table 4).

Arterial Blood IPPA Clearance

IPPA activity cleared rapidly from the arterial blood, falling below 35% ± 2% and 10% ± 1% of peak activity at 2 and 10 min after injection, respectively.

Serial IPPA SPECT Image Analysis

Ischemic-to-nonischemic ratios of myocardial IPPA activity were obtained from selected SPECT images in all 9 dogs without infarction. These results are summarized in Figure 5. There was significant normalization of the ischemic defect ratio within 16 min of injection and nearly complete normalization within 48 min.

A complete series of in vivo SPECT images was available in only 6 of 9 dogs without infarction because of technical failures in the serial SPECT acquisitions. One of the 6 dogs was excluded from the analysis of regional myocardial IPPA clearance because this dog was an extreme outlier, showing markedly delayed clearance from ischemic and nonischemic regions in association with significant hypotension.

Serial short-axis SPECT IPPA images from a representative dog are shown in Figure 6A. Significant normalization of the defect occurred early after IPPA injection. Myocardial time–activity curves derived from ischemic and nonischemic regions are shown in Figure 6B for this same dog. The early clearance data for the same dog are also displayed as a semilogarithmic plot (Fig. 6C). The early myocardial clearance appears linear on this plot, suggesting early monoexponential clearance of IPPA. Early (8–36 min) myocardial IPPA clearance from the ischemic region ($t_{1/2}$ = 54.2 ± 3.3 min) was significantly longer than that from nonischemic region ($t_{1/2}$ = 36.7 ± 5.6 min; n = 5 dogs, $P < 0.05$). These results are summarized in Table 5.

Myocardial IPPA and ^{18}F-FDG Activity

The retained IPPA and ^{18}F-FDG activities in all myocardial segments were normalized to activity in the control nonischemic region. Myocardial segments were segregated on the basis of normalized flow into 20%-flow intervals (Fig. 7). The retained myocardial IPPA and ^{18}F-FDG activities were increased significantly in all regions with mild (60%–80% of the nonischemic region) to moderate (40%–60% of the nonischemic region) reductions in flow. However, the greatest increase in relative myocardial IPPA and ^{18}F-FDG activities occurred in ischemic segments with moderate reductions of blood flow (40%–60% of the nonischemic region). The maximal increase in the ischemic myocardial IPPA activity was 151% ± 9.7% of the non-

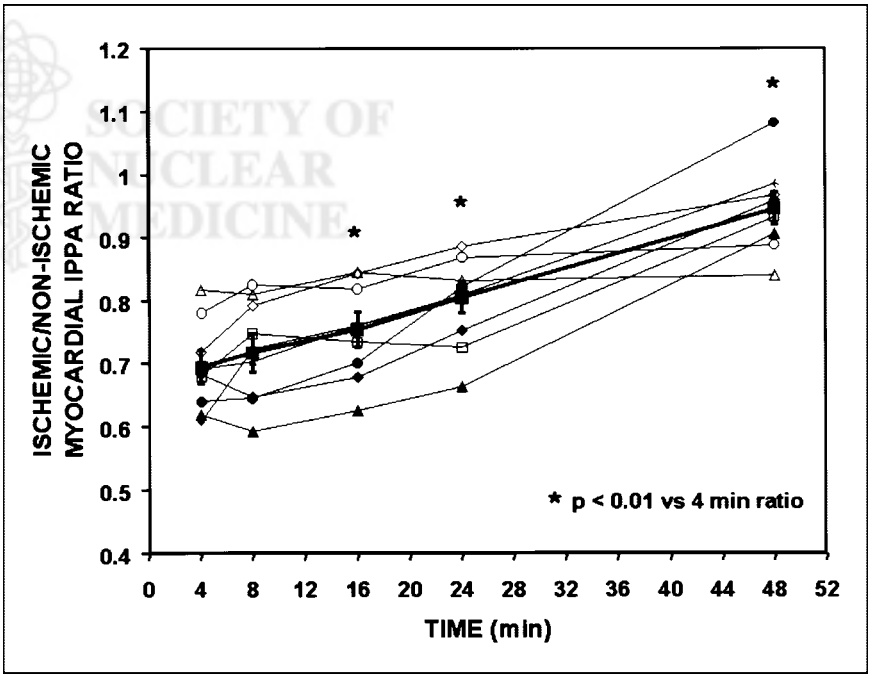

FIGURE 5. Ischemic-to-nonischemic ratios of myocardial IPPA activity obtained in 9 dogs from selected IPPA SPECT images. Individual dogs are represented by different symbols. Average ratio is represented by ■ and thickened line. Significant normalization of ischemic defect ratio occurred within 16 min and nearly complete normalization of defect ratio occurred within 48 min after injection. Data are expressed as mean ± SEM.

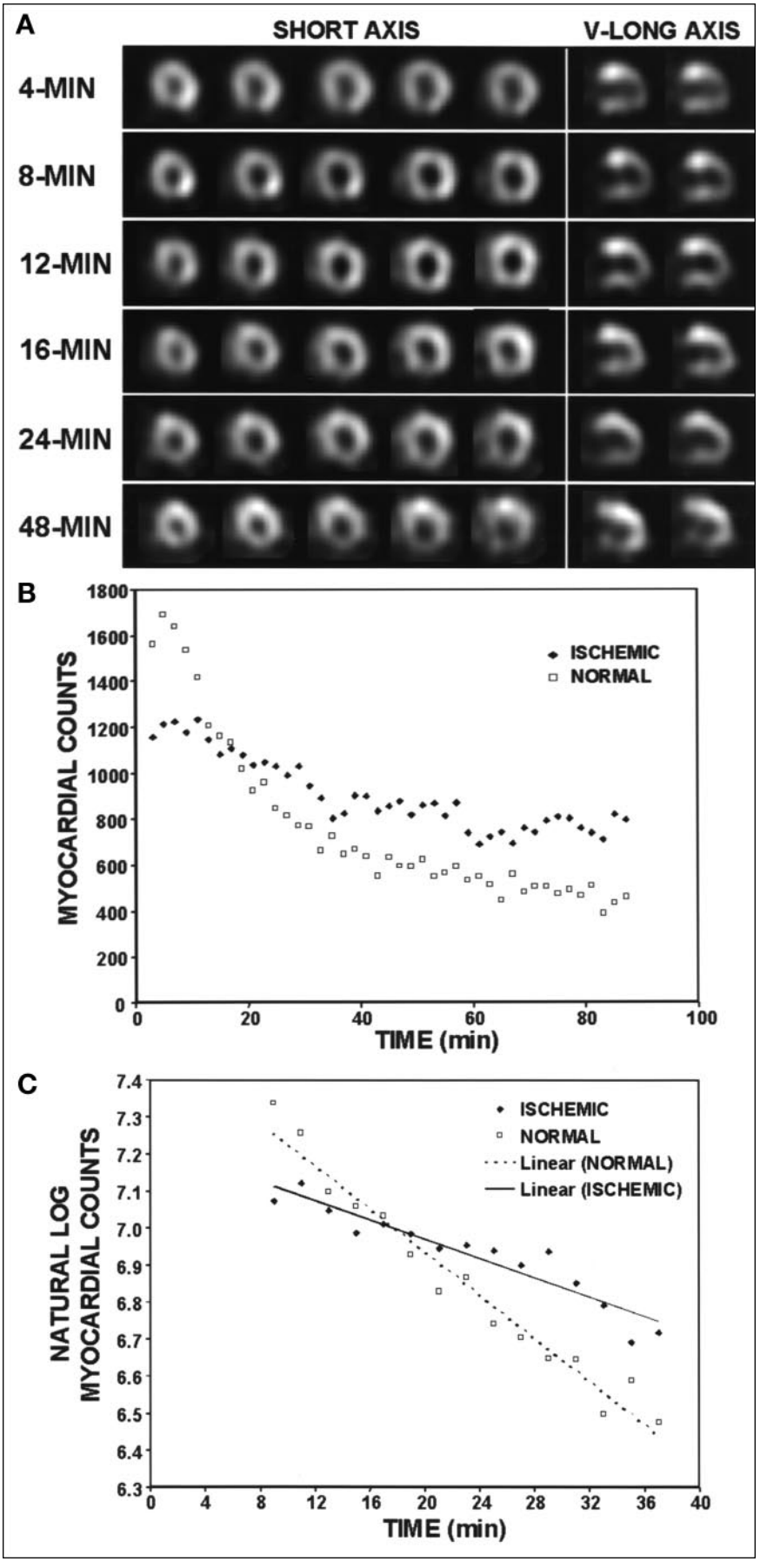

FIGURE 6. (A) Serial short-axis and vertical long (v-long) axis SPECT IPPA images from representative dog displayed in standard format. Time after injection is designated on left margin. Note perfusion defect in anteroseptal and anteroapical regions, which normalizes over time. (B) Myocardial IPPA clearance curves derived from ischemic and nonischemic regions for same dog. (C) Early clearance data for same dog are also displayed as semilogarithmic plot. Early myocardial clearance appears linear on this semilogarithmic plot, suggesting early monoexponential clearance of IPPA. Delayed myocardial IPPA clearance is seen in ischemic region.

TABLE 5
Myocardial IPPA Clearance Half-Time ($t_{1/2}$) for Nonischemic (LCX) and Ischemic (LAD) Regions

Dog no.	LCX $t_{1/2}$ (min)	LAD $t_{1/2}$ (min)
1	29.7	57.6
2	54.5	60.0
3	21.9	57.1
4	48.6	57.0
5	28.8	39.4
Mean ± SEM*	36.7 ± 5.6	54.2 ± 3.3†

*n = 5 dogs.
†$P < 0.05$ vs. LCX.
One dog was excluded from analysis because of abnormal clearance in control region possibly attributed to profound hypotension.

ischemic activity. A greater increase in the ischemic myocardial ^{18}F-FDG activity was observed for all flow ranges. The maximal increase in myocardial ^{18}F-FDG activity was 450% ± 47% of the nonischemic activity.

Overall, a fair correspondence ($r = 0.70$, $P < 0.0001$) was found between normalized myocardial IPPA and ^{18}F-FDG activities ($n = 576$ segments, 6 dogs). The variability among individual dogs led to a relatively large SEE of 126 in the pooled analysis. A significant correlation was found between myocardial IPPA and ^{18}F-FDG activities in each individual dog, although the correlation coefficients were quite variable, ranging from 0.33 to 0.97. These data are summarized in Figure 8.

DISCUSSION

Several findings in this study indicate that IPPA SPECT imaging may be useful for noninvasive detection of myocardial ischemia. Analysis of serial in vivo SPECT IPPA images showed that low-flow ischemia results in a delay in early clearance of IPPA from the ischemic myocardium. In addition, relative myocardial retention of IPPA in the ischemic myocardium was increased 130 min after injection, particularly in regions of mild-to-moderate flow reduction, secondary to differential clearance between ischemic and normal regions. Regional differences in myocardial IPPA clearance were associated with alterations in myocardial substrate utilization and the increased relative myocardial IPPA retention. The increased relative myocardial retention of IPPA in ischemic regions also correlated with ^{18}F-FDG accumulation.

Although previous studies have evaluated the uptake and clearance characteristics of IPPA under conditions of myocardial infarction or ischemia (*19,30–32*), this study represents the first experimental study to evaluate absolute myocardial IPPA clearance under conditions of sustained low-flow ischemia in comparison with ^{18}F-FDG accumulation.

We used an acute in vivo canine model of sustained low-flow myocardial ischemia, which produced a 55% reduction of relative endocardial flow and a 30% reduction in transmural flow in the central ischemic region. This degree of flow restriction resulted in a profound reduction in regional myocardial thickening. Low-flow ischemia was associated with a change in substrate utilization. A switch to anaerobic metabolism occurred, which was verified by lac-

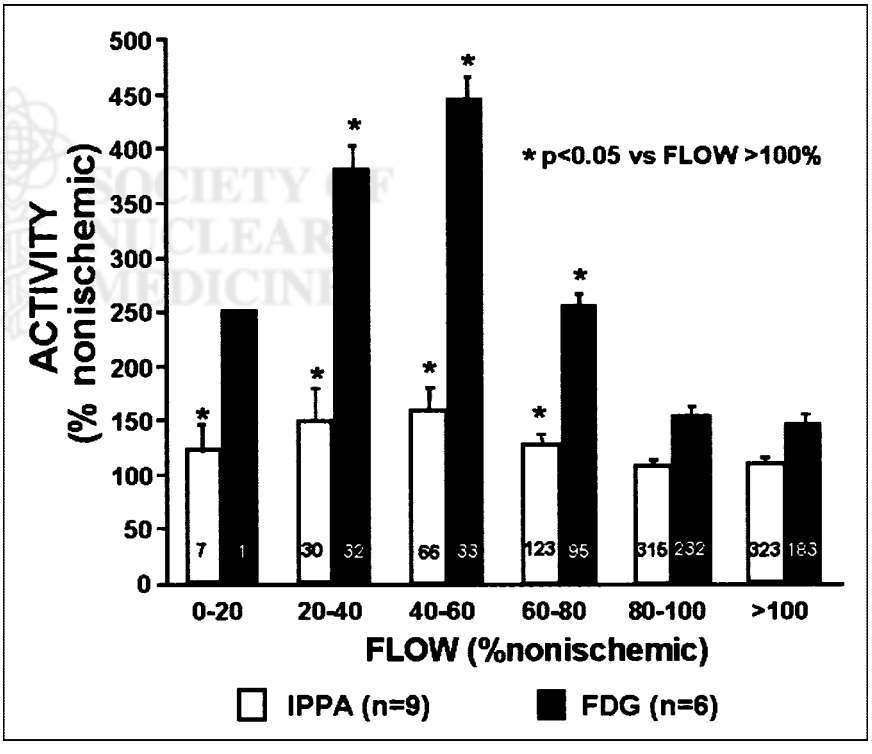

FIGURE 7. Myocardial IPPA and ^{18}F-FDG retained activities expressed as nonischemic percentage for all segments (n = 576). Segments were segregated on basis of normalized flows in segments into 20%-flow increments. Numbers within each bar represent number of segments falling into each flow range.

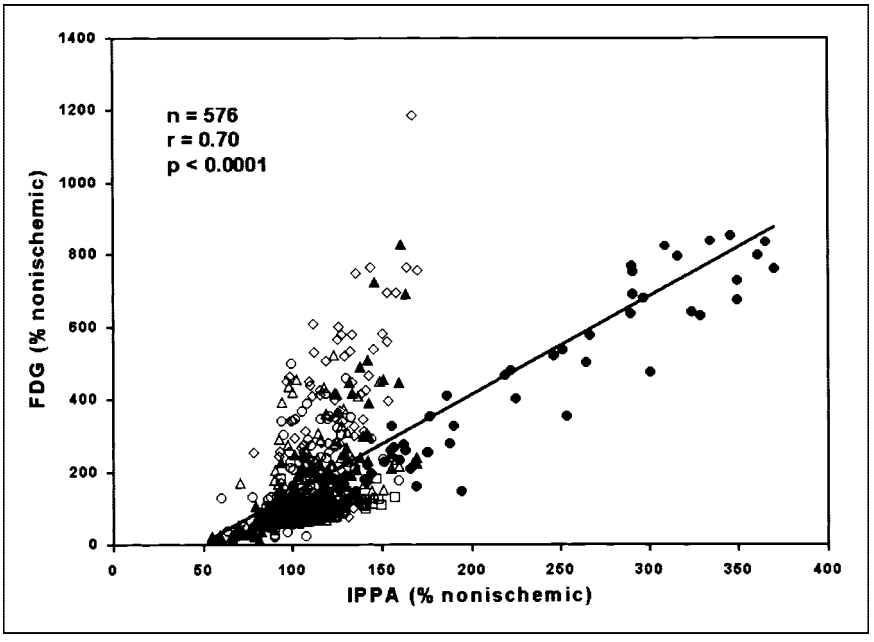

FIGURE 8. Correlation between normalized myocardial IPPA and ^{18}F-FDG retained activity for all dogs (n = 6) injected with ^{18}F-FDG. Individual dogs are represented by different symbols.

tate production in the central ischemic region, decreased extraction of FFA, and reduction in oxygen consumption in the ischemic region.

We observed an initial IPPA SPECT defect reflecting reduced initial delivery and decreased FFA uptake in the ischemic region. This finding is consistent with the report by Reske et al. (*31*) in which myocardial blood flow and initial myocardial IPPA uptake were closely related in normal and in acutely ischemic myocardium. Caldwell et al. (*32*) also showed that the initial myocardial distribution of IPPA tracked flow linearly to high levels during treadmill exercise in conscious dogs.

However, myocardial retention of IPPA late (130 min) after injection was significantly increased, relative to that of the nonischemic control regions, in regions with a moderate flow reduction. Myocardial IPPA activity in the very-low-flow regions did not exceed that in the normal regions, probably because of reduced initial delivery. The observed early delayed clearance and increase in late myocardial IPPA retention in ischemic regions may have occurred as a consequence of several concurrent mechanisms.

First, the initial decreased clearance of IPPA from the ischemic myocardium is primarily attributed to decreased β-oxidation of FFAs. Although we did not directly measure β-oxidation, we found that steady-state FFA uptake and oxygen consumption were reduced during sustained low-flow ischemia. Schön et al. (*4*) reported delayed early clearance of ^{11}C-palmitic acid by ischemic myocardium, which was also related to oxygen consumption. Reske et al. (*9*) found that initial cardiac uptake and clearance of IPPA and 1-^{14}C-palmitic acid paralleled each other in murine tissues, further supporting the idea that early IPPA clearance reflects β-oxidation of FFAs.

Second, changes in tissue intermediates associated with regional ischemia inhibit β-oxidation of long-chain acyl coenzyme A with an increase in esterification to triacylglycerols (*21*). Several investigators have shown that fatty acid esterification to triacylglycerols exceeds lipolysis during myocardial ischemia (*33*,*34*). The increased late retention of IPPA probably reflects incorporation of IPPA into triglyceride pools, with a slow late clearance from this pool (*35*,*36*).

Rellas et al. (*30*) observed reduced myocardial IPPA clearance in experimental models of permanent coronary occlusion and occlusion-reperfusion. This study suggested that cardiac metabolic imaging with IPPA was useful for discrimination of postischemic viable myocardium and infarcted myocardium. However, their analysis of myocardial IPPA clearance was restricted to relative regional washout from a sparse series of images and did not include regional metabolic measurements as obtained in our study. In our canine model of acute low-flow ischemia, quantitative analysis of serial IPPA SPECT imaging was able to discriminate low-flow ischemic regions from normal regions. In addition to the analysis of relative myocardial activity or differential clearance, we showed delayed absolute myocardial IPPA clearance from the ischemic region relative to that of the nonischemic region using monoexponential fitting of the early (8–36 min) phase of myocardial clearance.

In a pilot clinical study of IPPA SPECT imaging for the evaluation of myocardial viability in patients referred for coronary revascularization, Hansen et al. (*15*,*16*) performed serial IPPA SPECT imaging before and 8 wk after coronary revascularization. These investigators assumed monoexponential clearance of IPPA similar to our analysis. They also restricted their analysis to the initial early clearance phase

(4–36 min after injection), the clearance phase that is thought to reflect primarily β-oxidation. This clinical study showed delayed myocardial clearance of IPPA in chronically ischemic hibernating regions.

^{18}F-FDG is the most widely used tracer for studying myocardial metabolism and is an established marker of myocardial viability (*1*,*2*). The inverse relationship between ^{18}F-FDG retention and blood flow has been well described (*37*,*38*). Metabolic activity is maintained if the flow is reduced by 40%–60% of normal but is severely diminished if blood flow is further reduced by >70%–80% of that in the normal myocardium (*37*,*38*). In our acute low-flow study, we observed, on average, an approximately 3-fold increase in ^{18}F-FDG accumulation in the ischemic region. This increase was similar to the 3-fold increase in transmural glucose uptake in the ischemic region, which we reported earlier in this model (*22*). Fallavollita et al. (*39*) reported an approximately 2-fold increase in myocardial ^{18}F-FDG uptake, under conditions of chronic ischemia (approximately 12% reduction in transmural microsphere flow), produced by implantation of an LAD ameroid occluder in pigs.

In this study, we directly compared myocardial IPPA retention at 130 min after injection with ^{18}F-FDG accumulation (40 min after injection) under conditions of sustained low-flow ischemia and showed a fair ($r = 0.70$) correlation of myocardial IPPA and ^{18}F-FDG activities. This finding further supports the use of IPPA for detection of ischemic myocardium, although the retention of IPPA was not as high as that observed for ^{18}F-FDG. It is possible that the retention may have been higher and the correlation between relative myocardial IPPA and ^{18}F-FDG activities may have been better if both tracers were injected simultaneously, at identical levels of myocardial ischemia.

This study has several limitations that need to be considered. Our protocol was designed to study the kinetics of IPPA using serial SPECT imaging and to examine subsequent myocardial IPPA retention relative to that of ^{18}F-FDG. Serial IPPA SPECT images were acquired before injection of ^{18}F-FDG to evaluate the myocardial clearance of IPPA in the absence of tracer cross talk. In addition, dogs were killed 40 min after injection of ^{18}F-FDG to allow adequate time for myocardial ^{18}F-FDG accumulation. Therefore, the final myocardial distribution of IPPA as determined by γ-well counting does not correspond with the final IPPA SPECT imaging data. Under this protocol IPPA and ^{18}F-FDG were not injected simultaneously, making it more difficult to compare the myocardial distribution of these 2 metabolic tracers. However, there was no evidence of a significant change in regional myocardial flow or metabolism during the 90 min between the 2 injections. Hemodynamic parameters, FFA uptake, and lactate production all remained stable between the injections of IPPA and ^{18}F-FDG.

We used an acute canine model of sustained low-flow ischemia, which differs from chronic hibernating myocardium in patients. As with all acute open-chest experimental preparations, the potential confounding effects of anesthesia must be considered. The magnitude of the flow reduction in our study was also more severe than that in experimental studies of more chronic ischemia (*15*,*16*). In fact, 2 of the dogs deteriorated slightly over time under these ischemic conditions. One of these dogs showed myocardial necrosis on postmortem histochemical staining, after 190 min of low-flow ischemia.

Analysis of IPPA SPECT time–activity curves does not unambiguously define the metabolic fate of IPPA. The myocardial clearance rate cannot be used as a direct measure of β-oxidation because of the potential confounding effect of clearance of nonmetabolized IPPA (backdiffusion) and the potential confounding effects of flow. Nonetheless, serial IPPA SPECT imaging did permit the noninvasive identification of regional myocardial ischemia.

CONCLUSION

In our acute canine model of low-flow ischemia, we observed early delayed myocardial clearance of IPPA from ischemic regions and increased late relative myocardial retention of IPPA, which paralleled the accumulation of ^{18}F-FDG, supporting the use of serial IPPA SPECT imaging as a noninvasive approach for rapid detection of resting myocardial ischemia. We observed a more dramatic increase in relative myocardial ^{18}F-FDG accumulation relative to that of IPPA retention, suggesting that serial IPPA SPECT imaging may not be as good as ^{18}F-FDG SPECT imaging for identification of resting ischemia. However, IPPA SPECT imaging would not require the availability of a cyclotron or special high-energy SPECT imaging equipment as required for ^{18}F-FDG SPECT imaging.

Our findings also suggest that serial IPPA SPECT imaging can detect resting ischemic myocardium within 36 min of radiotracer injection, by analysis of changes in either the myocardial defect ratio or the regional myocardial clearance using simple monoexponential curve fitting. Late redistribution imaging, 3-4 h after injection, may not be required for detection of resting ischemia, as required with rest-redistribution ^{201}T1 imaging. We speculate that quantitative estimation of myocardial IPPA clearance from serial IPPA SPECT images may provide a better estimation of regional ischemia because this approach may avoid the potential problem of detecting ischemia in the presence of multivessel disease or balanced ischemia. However, clinical trials evaluating the potential role of serial IPPA SPECT imaging for the rapid assessment of myocardial ischemia in patients with multivessel disease seem warranted. The potential confounding effects of myocardial necrosis on myocardial IPPA clearance also warrant further investigation.

ACKNOWLEDGMENTS

The authors gratefully acknowledge the assistance of Dr. James A. Arrighi, Dr. Xiao-Yu Hu, Dr. Chin K. Ng, Donald

P. Dione, Wendy Bruni, Donna Natale, Syed Hasan, and Paul DeMan. This research was supported by a grant from Medco Research Co. and by a grant-in-aid and a fellowship award from the Connecticut Affiliate of the American Heart Association.

REFERENCES

1. Tillisch J, Brunken R, Marshall R, et al. Reversibility of cardiac wall motion abnormalities predicted by positron tomography. *N Engl J Med*. 1986;314:884–888.
2. Tamaki N, Yonekura Y, Yamashita K, et al. Positron emission tomography using fluorine-18 deoxyglucose in evaluation of coronary artery bypass grafting. *Am J Cardiol*. 1989;64:860–865.
3. Lerch R, Ambos H, Bergmann S, et al. Localization of viable, ischemic myocardium by positron-emission tomography with ^{11}C-palmitate. *Circulation*. 1981; 64:689–699.
4. Schön H, Schelbert H, Najafi A, et al. C-11 labeled palmitic acid for the noninvasive evaluation of regional myocardial fatty acid metabolism with positron-computed tomography. II. Kinetics of C-11 palmitic acid in acutely ischemic myocardium. *Am Heart J*. 1982;103:548–561.
5. Schelbert HR, Henze E, Schon HR, et al. C-11 palmitate for the noninvasive evaluation of regional myocardial fatty acid metabolism with positron-computed tomography. III. In vivo demonstration of the effects of substrate availability on myocardial metabolism. *Am Heart J*. 1983;105:492–504.
6. Rosamond T, Abendschein D, Sobel B, et al. Metabolic fate of radiolabeled palmitate in ischemic canine myocardium: implications for positron emission tomography. *J Nucl Med*. 1987;28:1322–1329.
7. Machulla H, Dutschka K, Van Beuningen D, Chen T. Development of 15-(p-123-I-phenyl)-pentadecanoic acid for in vivo diagnosis of the myocardium. *J Radioanal Chem*. 1981;65:279–286.
8. Machulla H, Knust E, Vyska K. Radioiodinated fatty acids for cardiological diagnosis. *Int J Radiat Appl Instrum [A]*. 1986;37:777–788.
9. Reske S, Sauer W, Machulla H, Winkler C. 15(p-[I-123]Iodophenyl) pentadecanoic acid as tracer of lipid metabolism: comparison with (1-14C) palmitic acid in murine tissues. *J Nucl Med*. 1984;25:1335–1342.
10. Hansen C, Corbett J, Pippin J, et al. Iodine-123 phenylpentadecanoic acid and single photon emission computed tomography in identifying left ventricular regional metabolic abnormalities in patients with coronary heart disease: comparison with thallium-201 myocardial tomography. *J Am Coll Cardiol*. 1988;12: 78–87.
11. Vyska K, Machulla H, Stremmel W, et al. Regional myocardial free fatty acid extraction in normal and ischemic myocardium. *Circulation*. 1988;78:1218–1233.
12. Reske S, Knapp FJ Jr, Winkler C. Experimental basis of metabolic imaging of the myocardium with radioiodinated aromatic free fatty acids. *Am J Physiol Imaging*. 1986;1:214–229.
13. Kennedy P, Corbett J, Kulkarni P, et al. I-123 phenylpentadecanoic acid myocardial scintigraphy: usefulness in identifying myocardial ischemia. *Circulation*. 1986;74:1007–1015.
14. Walamies M, Turjanmaa V, Koskinen M, Uusitalo A. Diagnostic value of ^{123}I-phenylpentadecanoic acid (IPPA) metabolic and thallium 201 perfusion imaging in stable coronary artery disease. *Eur Heart J*. 1993;14:1079–1087.
15. Hansen C. Preliminary report of an ongoing phase I/II dose range, safety and efficacy study of iodine-123-phenylpentadecanoic acid for the identification of viable myocardium. *J Nucl Med*. 1994;35(suppl):38S–42S.
16. Hansen C, Heo J, Oliner C, et al. Prediction of improvement in left ventricular function with iodine-123-IPPA after coronary revascularization. *J Nucl Med*. 1995;36:1987–1993.
17. Iskandrian A, Powers J, Cave V, et al. Assessment of myocardial viability by dynamic tomographic 123-I-iodophenylpentadecanoic acid imaging: comparison to rest-redistribution thallium-201 imaging. *J Nucl Cardiol*. 1995;2:101–109.
18. Verani MS, Taillefer R, Iskandrian AE, et al. ^{123}I-IPPA SPECT for the prediction of enhanced left ventricular function after coronary bypass graft surgery: Multicenter IPPA Viability Trial Investigators—^{123}I-iodophenylpentadecanoic acid. *J Nucl Med*. 2000;41:1299–1307.
19. Yang J, Ruiz M, Calnon D, et al. Assessment of myocardial viability using ^{123}I-labeled iodophenylpentadecanoic acid at sustained low flow or after acute infarction and reperfusion. *J Nucl Med*. 1999;40:821–828.
20. Opie L. Metabolic response during impending myocardial infarction. I. Relevance of studies of glucose and fatty acid metabolism in animals. *Circulation*. 1972;45:483–490.
21. Whitmer J, Idell-Wenger J, Rovetto M. Control of fatty acid metabolism in ischemic and hypoxic hearts. *J Biol Chem*. 1978;253:4305–4309.
22. Young L, Renfu Y, Russel R, et al. Low-flow ischemia leads to translocation of canine heart GLUT-4 and GLUT-1 glucose transporters to the sarcolemma in vivo. *Circulation*. 1997;95:415–422.
23. Shi C, Sinusas A, Dione D, et al. Technetium-99m-nitroimidazole (BMS181321): a positive imaging agent for detecting myocardial ischemia. *J Nucl Med*. 1995; 36:1078–1086.
24. Edwards N, Sinusas A, Bergin J, et al. Influence of subendocardial ischemia on transmural myocardial function. *Am J Physiol*. 1992;262:H568–H576.
25. Sinusas A, Watson D, Cannon J, Beller G. Effect of ischemia and postischemic dysfunction on myocardial uptake of ^{99m}Tc-labeled methoxy isobutyl isonitrile and ^{201}Tl. *J Am Coll Cardiol*. 1989;14:1785–1793.
26. Miles J, Glasscock R, Aikens J, et al. A microfluorometric method for the determination of free fatty acids in plasma. *J Lipid Res*. 1983;24:96–99.
27. Kulkarni P, Parkey P. A new radioiodination method utilizing organothallium intermediate radioiodination of phenyl pentadecanoic acid (PPA) for potential applications in myocardial imaging [abstract]. *J Nucl Med*. 1982;23(suppl):P105.
28. Liu Y, Sinusas A, Shi C, et al. Quantitation of technetium 99m-labeled sestamibi SPECT based upon mean counts improves accuracy for assessment of relative blood flow: experimental validation in a canine model. *J Nucl Cardiol*. 1996;3: 312–320.
29. Liu Y, Sinusas A, DeMan P, et al. Quantification of single photon emission computerized tomographic myocardial perfusion images: methodology and validation of the Yale-CQ method. *J Nucl Cardiol*. 1999;6:190–204.
30. Rellas J, Corbett J, Kulkarni P, et al. Iodine-123-phenylpentadecanoic acid: detection of acute myocardial infarction and injury in dogs using an iodinated fatty acid and single photon emission tomography. *Am J Cardiol*. 1983;52:1326–1332.
31. Reske S, Schon N, Knust E, et al. Relation of myocardial blood flow and initial cardiac uptake of 15-(p-^{123}I-phenyl)-pentadecanoic acid in the canine heart. *Nuklearmedizin*. 1984;23:83–85.
32. Caldwell J, Martin G, Link J, et al. Iodophenylpentadecanoic acid-myocardial blood flow relationship during maximal exercise with coronary occlusion. *J Nucl Med*. 1990;30:99–105.
33. Scheuer J, Brachfeld N. Myocardial uptake and fractional distribution of palmitate-I-C^{14} by the ischemic dog heart. *Metabolism*. 1966;15:945–954.
34. Lochner A, Kotze J, Benade A. Mitochondrial oxidative phosphorylation in low-flow hypoxia: role of free fatty acids. *J Mol Cell Cardiol*. 1978;10:857–875.
35. Reske S, Sauer W, Machulla H, et al. Metabolism of 15(p-123-I-iodophenyl-) pentadecanoic acid in heart muscle and noncardiac tissue. *Eur J Nucl Med*. 1985;10:228–234.
36. van der Wall EE. Myocardial imaging with radiolabeled free fatty acids: applications and limitations. *Eur J Nucl Med*. 1986;12:S11–S15.
37. Sochor H, Schwaiger M, Schelbert H, et al. Relationship between Tl-201, Tc-99m (Sn) pyrphosphate and F-18 2-dexyglucose uptake in ischemically injured dog myocardium. *Am Heart J*. 1987;114:1066–1077.
38. Kaliff V, Schwaiger M, Nguyen N, et al. The relationship between myocardial blood flow and glucose uptake in ischemic canine myocardium determined with fluorine-18-deoxyglucose. *J Nucl Med*. 1992;33:1346–1353.
39. Fallavollita J, Perry B, Canty JJ. ^{18}F-2-Deoxyglucose deposition and regional flow in pigs with chronically dysfunctional myocardium: evidence for transmural variation in chronic hibernating myocardium. *Circulation*. 1997;95:1900–1909.